# A Geometrical Interpretation of Force and Position Constraints in the Optimal Control of Wave Energy Devices

Giorgio Bacelli
Center for Ocean Energy Research
Department of Electronic Engineering
National University of Ireland Maynooth, Ireland
E-mail: gbacelli@eeng.nuim.ie

John V. Ringwood
Center for Ocean Energy Research
Department of Electronic Engineering
National University of Ireland Maynooth, Ireland
E-mail: john.ringwood@eeng.nuim.ie

***Abstract*—Physical constraints need to be considered in the design of control systems for an oscillating body Wave Energy Converter (WEC). In the case of a hydraulic Power Take Off (PTO) unit, such constraints include the length of the stroke of a hydraulic piston or the maximum pressure permitted in the hydraulic circuit. In the paper, two types of WEC are considered: A 1-body point absorber oscillating in heave and a 2-body point absorber also oscillating in heave. A procedure for the analysis of the constraints is presented. It provides sufficient conditions for the satisfaction of both constraints and/or the violation of at least one constraint. The procedure is based on the discretization of the equations of motion of the WECs by approximating the forces and the velocities with a linear combination of basis functions. A special case is presented in which truncated Fourier series are used for the approximation. It is shown that the constraints can be interpreted as a geometrical object in a finite dimensional vector space, and that the study of sufficient conditions for the satisfaction of both constraints and for sufficient conditions for the violation of at least one constraint can be seen as the study of the intersection between these geometrical objects. It is also shown that the method allows the study of the effect of constraints on the amount of produced energy.**

***Index Terms*—WEC, Single body, Self reacting, Control, Constraints.**

## I. Introduction

The design of Wave Energy Converters (WECs) requires the analysis of constraints introduced by physical limitations of the components used to build the device. For a heaving buoy point absorber, which is considered in this paper, examples of such limitations are the maximum force that the Power Take Off (PTO) unit can exert and the maximum amplitude of its oscillation. The analysis of constraints is important not only with respect to the maximum amount of energy that the device can produce, but also for the study of the survivability of the WEC to a specific wave climate. For example, the amplitude of the relative motion, between the two bodies composing the self-reacting heaving buoy point absorber in Fig 1, depends on the excitation force and on the force applied by the PTO. Each body composing the WEC is subject to a different excitation force; if the difference is large, the PTO may not be able to keep the relative motion within the limits, risking damage to the device.

The method presented in this paper provides a tool that can be used in the design stage of a WEC to quickly analyze the physical requirements on the PTO force and on the oscillation amplitude as function of the sea state. In particular, it provides sufficient conditions for the satisfaction of both force and amplitude constraints, and sufficient conditions for the violation of at least one of the constraints.

The procedure is based on the discretization of the equations of motion of the WECs by means of the approximation of the forces and of the velocities with a linear combination of basis functions. A special case is considered, in which truncated Fourier series are used for the approximation. This case is particularly interesting because the results are in strict analogy with the frequency domain theory of wave energy conversion, as in [1]. The discretization was initially motivated by the study of an optimal controller for the maximization of the energy converted by the device, subject to constraints. Only the details crucial to the development of the constraint framework are described here. The full details of the underlying control framework are given in [2].

Two types of WECs are considered: a two-body self-reacting point absorber restricted to heave motion, which is depicted in Fig. 1, and a single body point absorber restricted to heave motion, which is considered as a particular case of the two-body device.

The two-body device is considered in Section II; both frequency and time domain models are presented to introduce the terminology that will be used through the rest of the paper. In Section II-A the discretization of the time domain model is described, at first using general basis functions for the approximation of the forces and velocities, and subsequently truncated fourier series are considered. In Section II-B, force and amplitude constraints are defined using the infinity norm and then approximated by the 2-norm. The introduction of the 2-norm is motivated by the fact that it allows the analytical formulation of some useful results that will be used in Section II-C to study conditions for the satisfaction and/or violation of constraints. The single body WEC is considered in Section III as a particular case of the two-body device.

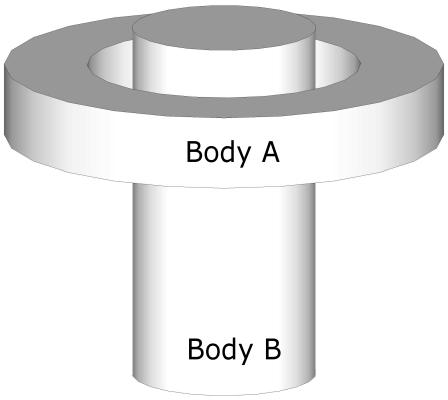


Fig. 1. Self-reacting point absorber.

Section IV provides the example of a vertical cylinder with the step by step description of the practical implementation of the method, and a discussion concerning the effect of constraints on the amount of converted energy.

## II. Self-reacting point absorber

The general form of device considered is a two-body self-reacting point absorber restricted to heave motion only, as depicted in Fig. 1, and described by the frequency domain model [3]:

$$\begin{cases} \left(i\omega\, m^A + B^A + \dfrac{S^A}{i\omega}\right) V^A = F_e^A + F_r^A - F_{pto} \\ \left(i\omega\, m^B + B^B + \dfrac{S^B}{i\omega}\right) V^B = F_e^B + F_r^B + F_{pto} \end{cases} \tag{1}$$

where $V^A$ and $V^B$ are the vertical velocities of body $A$ and body $B$, respectively. The radiation force $F_r$ is

$$\begin{bmatrix} F_r^A \\ F_r^B \end{bmatrix} = -Z \begin{bmatrix} V^A \\ V^B \end{bmatrix} \text{ with } Z = \begin{bmatrix} Z^{AA} & Z^{AB} \\ Z^{BA} & Z^{BB} \end{bmatrix}$$

where $Z$=$Z(\omega)$ is the radiation impedance matrix. $F_e^B$ and $F_e^B$ denote the excitation forces, $m^A$ and $m^B$ are the masses, $S^A$ and $S^B$ the hydrodynamic stiffness, $B^A$ and $B^B$ are damping coefficients used to model linear losses due to viscous effects and frictions of mechanical components. The PTO applies a force $F_{pto}$ on both bodies with the same magnitude and opposite direction. The time domain formulation of the model in Equation 1 is

$$\begin{cases} L^A(t) = m^A \dot{v}^A(t) + B^A v^A(t) + S^A u^A(t) \\ \qquad\qquad - f_e^A(t) - f_r^A(t) + f_{pto}(t) = 0 \\ L^B(t) = m^B \dot{v}^B(t) + B^B v^B(t) + S^B u^B(t) \\ \qquad\qquad - f_e^B(t) - f_r^B(t) - f_{pto}(t) = 0 \end{cases} \tag{2}$$

where $u^A(t)$ and $u^B(t)$ are the vertical positions of the two bodies, and $\dot{v}^A(t)$ and $\dot{v}^B(t)$ their vertical accelerations. The forces and velocities, denoted with lowercase letters in Equation 2, are the inverse Fourier transform of the corresponding uppercase variables in equations 1. The radiation forces become

$$\begin{aligned} f_r^A(t) = &-m_\infty^{AA}\dot{v}^A(t) - k^{AA}(t) * v^A(t) \\ &- m_\infty^{AB}\dot{v}^B(t) - k^{AB}(t) * v^B(t) \end{aligned}$$

$$\begin{aligned} f_r^B(t) = &-m_\infty^{BB}\dot{v}^B(t) - k^{BB}(t) * v^B(t) \\ &- m_\infty^{BA}\dot{v}^A(t) - k^{BA}(t) * v^A(t) \end{aligned}$$

where the symbol $*$ denotes the convolution operator and the parameters $m_\infty^{ij}$ and $k^{ij}(t)$, with $i, j \in \{A, B\}$, are related to the elements of the radiation impedance matrix $Z$ through the expressions [4]:

$$\begin{aligned} m^{ij}(\omega) &= \text{Im}\{Z^{ij}(\omega)\} = m_\infty^{ij} - \frac{1}{\omega}\int_0^\infty k^{ij}(t)\, \sin(\omega t)\, dt, \\ R^{ij}(\omega) &= \text{Re}\{Z^{ij}(\omega)\} = \int_0^\infty k^{ij}(t)\, \cos(\omega t)\, dt, \\ m_\infty^{ij} &= \lim_{\omega\to\infty} \text{Im}\{Z^{ij}(\omega)\}. \end{aligned} \tag{3}$$

The energy absorbed in the interval $[0, T]$, neglecting the losses, corresponds to the work performed by the PTO, that is:

$$J(T) = \int_0^T f_{pto}(t)\,(v^A(t) - v^B(t))\, dt. \tag{4}$$

### A. Discretization

The PTO force is assumed to be such that $f_{pto}^{AB}(t) \in L^2([0, T])$, where $L^2([0, T])$ is the Hilbert space of square integrable functions in the interval $[0, T]$; also $v^A(t), v^B(t) \in L^2([0, T])$ because they are velocities of physical bodies. The PTO force and the velocities are then approximated as a linear combination of basis functions in a finite dimensional subspace of the space $L^2([0, T])$:

$$v^i(t) \approx \hat{v}^i(t) = \sum_{n=1}^{N} x_n^i\, \phi_n(t), \quad i \in \{A, B\} \tag{5}$$

$$f_{pto}(t) \approx \hat{f}_{pto}(t) = \sum_{n=1}^{N^P} p_n\, \phi_n^P(t) \tag{6}$$

where $\{\phi_1(t), \ldots, \phi_N(t)\}$ is a basis for the finite dimensional subspace $S^V \subset L^2([0, T])$ and $\{\phi_1^P(t), \ldots, \phi_{N^P}^P(t)\}$ is a basis for the finite dimensional subspace $S^P \subset L^2([0, T])$. For any given set of coefficients describing the PTO force $\{p_1, \ldots, p_{N^P}\}$ and excitation forces $f_e^A$ and $f_e^B$, the components of the velocities are calculated by applying the Galerkin method [5]:

$$\begin{cases} \langle \hat{L}^A(t), \phi_n \rangle = 0 \\ \langle \hat{L}^B(t), \phi_n \rangle = 0 \end{cases} \quad \forall\, n = 1, \ldots, N \tag{7}$$

where $\langle \cdot, \cdot \rangle$ denotes the inner product defined as

$$\langle f, g \rangle = \int_0^T f(t) g(t)\, dt, \tag{8}$$

and $\hat{L}^A(t)$ and $\hat{L}^B(t)$ are the equations of motion in the System 2 with the velocities and the forces approximated by

using Equations 5 and 6. The Galerkin method is a projection method for the discretization of integral and differential equations; the solution of Equation 7 is the set of the velocities components $x_n^i$ that minimizes the difference between the original equations of motion ($L^A$, $L^B$) and their approximation ($\hat{L}^A$ and $\hat{L}^B$). In other words, for any given PTO force and excitation forces, the solution of the Equation 7 provides the best approximation of the motion of the WEC in terms of the velocities components.

Given the oscillatory nature of the problem, a truncated Fourier series, also known as a trigonometric polynomial, is an intuitive choice as the basis for $S^V$ and $S^P$. Furthermore, choosing $w_0$=2$\pi/T$, the set of functions $\{\sin(\omega_0\, T)$, $\cos(\omega_0\, T),\ldots,\sin(N\omega_0\, T)$,$\cos(N\omega_0\, T)\}$ form an orthogonal basis for the spaces $S^V$ and $S^P$ with the inner product defined in Equation 8. The constant term of the basis is not considered because it is assumed that all the functions have zero mean; in practice, it is assumed that the reference frames of the bodies are chosen such that the origins oscillate around their mean position with respect to the inertial reference frame.

Using a zero mean truncated Fourier series with $N$ frequency components for both the velocities and the PTO force, the dimension of each of the spaces $S^V$ and $S^P$ is $2N$, and the resulting approximating functions in Equations 5 and 6 become:

$$\hat{v}^A(t) = \sum_{n=1}^{N} a_n^A \cos(n\omega_0 t) + b_n^A \sin(n\omega_0 t) \tag{9}$$

$$\hat{v}^B(t) = \sum_{n=1}^{N} a_n^B \cos(n\omega_0 t) + b_n^B \sin(n\omega_0 t) \tag{10}$$

$$\hat{f}_{pto}(t) = \sum_{n=1}^{N} a_n^P \cos(n\omega_0 t) + b_n^P \sin(n\omega_0 t). \tag{11}$$

For the practical implementation of the method, it is also convenient to approximate the excitation forces by a truncated Fourier series containing $N$ frequency components:

$$f_e^A(t) \approx \hat{f}_e^A(t) = \sum_{n=1}^{N} e_n^{A_c} \cos(n\omega_0 t) + e_n^{A_s} \sin(n\omega_0 t) \tag{12}$$

$$f_e^B(t) \approx \hat{f}_e^B(t) = \sum_{n=1}^{N} e_n^{B_c} \cos(n\omega_0 t) + e_n^{B_s} \sin(n\omega_0 t). \tag{13}$$

The mean value of the excitation forces can be considered to be zero with no loss of generality. In fact, since the excitation force is calculated by the convolution of the wave elevation with the excitation force kernel [3], the wave elevation can be transformed into a zero mean function by changing the origin of the reference frame, resulting in a zero mean excitation force.

Substituting Equations 9–13 into Equation 2, the system of Equations 7 becomes the linear system [2]:

$$\begin{bmatrix} G^{AA} & G^{AB} \\ G^{BA} & G^{BB} \end{bmatrix} \begin{bmatrix} X^A \\ X^B \end{bmatrix} = \begin{bmatrix} E^A \\ E^B \end{bmatrix} + \begin{bmatrix} -I_{2N} \\ I_{2N} \end{bmatrix} P \tag{14}$$

where $I_{2N}$ is the identity matrix of size $2N$,

$$\begin{aligned} X^A &= [a_1^A, b_1^A, a_2^A, b_2^A, \ldots, a_N^A, b_N^A]^T, \\ X^B &= [a_1^B, b_1^B, a_2^B, b_2^B, \ldots, a_N^B, b_N^B]^T, \\ E^A &= [e_1^{A_c}, e_1^{A_s}, e_2^{A_c}, e_2^{A_s}, \ldots, e_N^{A_c}, e_N^{A_s}]^T, \\ E^B &= [e_1^{B_c}, e_1^{B_s}, e_2^{B_c}, e_2^{B_s}, \ldots, e_N^{B_c}, e_N^{B_s}]^T, \\ P &= [a_1^p, b_1^p, a_2^p, b_2^p, \ldots, a_N^p, b_N^p]^T, \end{aligned}$$

$$G^{ij} = \begin{bmatrix} D_1^{ij} & M_1^{ij} & 0 & \cdots & 0 & 0 \\ -M_1^{ij} & D_1^{ij} & 0 & \cdots & 0 & 0 \\ 0 & 0 & \ddots & & \vdots & \vdots \\ \vdots & \vdots & & \ddots & 0 & 0 \\ 0 & 0 & \cdots & 0 & D_N^{ij} & M_N^{ij} \\ 0 & 0 & \cdots & 0 & -M_N^{ij} & D_N^{ij} \end{bmatrix}, \tag{15}$$

with $i, j$=$\{A, B\}$, and

$$D_n^{ii} = R^{ii}(n\omega_0) + B^i, \tag{16}$$

$$M_n^{ii} = n\omega_0 \left(m^i + m^{ii}(n\omega_0)\right) - S^i/(n\omega_0), \tag{17}$$

$$D_n^{ij} = R^{ij}(n\omega_0), \quad \text{for} \quad i \neq j \tag{18}$$

$$M_n^{ij} = n\omega_0\, m^{ij}(n\omega_0) \quad \text{for} \quad i \neq j. \tag{19}$$

The matrix $G_{ij}$ is block diagonal and each block is a 2-by-2 normal matrix of the form

$$\begin{bmatrix} a & b \\ -b & a \end{bmatrix}. \tag{20}$$

This particular structure is due to the orthogonality of the Fourier series and it allows the study of the existence of the solution of the linear system in Equation 14 by studying the singularity of each of the $N$ 4-by-4 matrices

$$G_n = \begin{bmatrix} D_n^{AA} & M_n^{AA} & D_n^{AB} & M_n^{AB} \\ -M_n^{AA} & D_n^{AA} & -M_n^{AB} & D_n^{AB} \\ D_n^{BA} & M_n^{BA} & D_n^{BB} & M_n^{BB} \\ -M_n^{BA} & D_n^{BA} & -M_n^{BB} & D_n^{BB} \end{bmatrix}. \tag{21}$$

Each matrix $G_n$ corresponds to a frequency $n\omega_0$; thus, should the system in Equation 14 be singular, a possible solution might be to perform a different frequency discretization by selecting a different fundamental frequency $\omega_0$.

If the solution of the linear system in Equation 14 exists, the amount of energy absorbed by the PTO, described by Equation 4, is

$$J(P) = -P^T H P + P^T (Q^A E^A - Q^B E^B) \tag{22}$$

where

$$\begin{aligned} H = S_{G^{BB}}^{-1} + {G^{AA}}^{-1} G^{AB} S_{G^{AA}}^{-1} \\ + {G^{BB}}^{-1} G^{BA} S_{G^{BB}}^{-1} + S_{G^{AA}}^{-1}, \end{aligned} \tag{23}$$

$$Q^A = S_{G^{BB}}^{-1} + {G^{BB}}^{-1} G^{BA} S_{G^{BB}}^{-1}, \tag{24}$$

$$Q^B = {G^{AA}}^{-1} G^{AB} S_{G^{AA}}^{-1} + S_{G^{AA}}^{-1}. \tag{25}$$

$S_{G^{AA}}$ and $S_{G^{BB}}$ are, respectively, the Schur complements of $G^{AA}$ and $G^{BB}$, and they are defined as

$$S_{G^{AA}} = G^{BB} - G^{BA}{G^{AA}}^{-1}G^{AB} \tag{26}$$

$$S_{G^{BB}} = G^{AA} - G^{AB}{G^{BB}}^{-1}G^{BA}. \tag{27}$$

It can be verified that the symmetric part of the matrix $H$ (i.e. $(H+H^T)/2$) is positive definite; therefore, the quadratic cost function in Equation 22 is concave and the global maximum of the unconstrained problem is obtained for

$$\bar{P} = (H+H')^{-1}(Q^A E^A - Q^B E^B). \tag{28}$$

### *B. Description and approximation of constraints*

The force constraint is defined as

$$\left\|\hat{f}_{pto}\right\|_\infty \leq F_{max}, \tag{29}$$

while the constraint on the relative amplitude is

$$\left\|\Delta\hat{u}\right\|_\infty \leq \Delta U_{max}, \tag{30}$$

where the infinity norm $\|\cdot\|_\infty$ is defined in the appendix (Equation 68) and $\Delta\hat{u}(t) = \hat{u}^A(t) - \hat{u}^B(t)$, with

$$\hat{u}^A(t) = u_0^A + \sum_{j=1}^{N} \frac{b_n^A}{n\omega_0}(1-\cos(n\omega_0 t)) + a_n^A \sin(n\omega_0 t), \tag{31}$$

$$\hat{u}^B(t) = u_0^B + \sum_{j=1}^{N} \frac{b_n^B}{n\omega_0}(1-\cos(n\omega_0 t)) + a_n^B \sin(n\omega_0 t). \tag{32}$$

Using the Inequality 69, it is possible to find sufficient conditions for the satisfaction of the Inequalities 29 and 30 in terms of the 2-norm, defined in the appendix (Equation 67):

$$\left\|\hat{f}_{pto}\right\|_\infty \leq \sqrt{\frac{2N}{T}}\left\|\hat{f}_{pto}\right\|_2 \leq F_{max}, \tag{33}$$

$$\left\|\Delta\hat{u}\right\|_\infty \leq \sqrt{\frac{2N}{T}}\left\|\Delta\hat{u}\right\|_2 \leq \Delta U_{max}. \tag{34}$$

The Inequalities 33 and 34 state that the 2-norm multiplied by $\sqrt{2N/T}$ is an upper bound for the infinity norm; as a consequence, if the inequality is satisfied for the 2-norm, it is also satisfied for the infinity norm. In practice, the condition on the 2-norm is more restrictive than the condition on the infinity norm.

Sufficient conditions for the violation of at least one of the constraints, also in terms of the 2-norm, can be obtained using the Inequality 70:

$$\left\|\hat{f}_{pto}\right\|_\infty \geq 1/\sqrt{T}\left\|\hat{f}_{pto}\right\|_2 \geq F_{max} \tag{35}$$

$$\left\|\Delta\hat{u}\right\|_\infty \geq 1/\sqrt{T}\left\|\Delta\hat{u}\right\|_2 \geq \Delta U_{max}. \tag{36}$$

The meaning of the Inequalities 35 and 36 is that the 2-norm multiplied by $1/\sqrt{T}$ is a lower bound for the infinity norm; thus, if the 2-norm multiplied by $1/\sqrt{T}$ violates the constraint, then the infinity norm also violates it.

The 2-norm of the force and amplitude constraints are calculated by applying Parseval's theorem, resulting in

$$\left\|\hat{f}_{pto}\right\|_2^2 = \frac{T}{2}\sum_{n=1}^{N}\left((a_n^p)^2 + (b_n^p)^2\right) = \frac{T}{2}P^T P, \tag{37}$$

$$\begin{aligned}\left\|\Delta\hat{u}\right\|_2^2 &= \frac{T}{2}\sum_{n=1}^{N}\frac{1}{n\omega_0}\left((b_n^A - b_n^B)^2 + (a_n^A - a_n^B)^2\right)\\ &= \frac{T}{2}(X^A - X^B)^T W^2 (X^A - X^B),\end{aligned} \tag{38}$$

where the amplitude constraint is obtained by setting the initial relative position $\Delta\hat{u}(0)$ as

$$\Delta\hat{u}(0) = \sum_{n=1}^{N}\frac{b_n^B - b_N^A}{n\omega_0}$$

to obtain a zero mean valued relative position, and the matrix $W$ is:

$$W = \begin{bmatrix} 1/\omega_0 & 0 & \cdots & 0 & 0 \\ 0 & 1/\omega_0 & \cdots & 0 & 0 \\ \vdots & \vdots & \ddots & \vdots & \vdots \\ 0 & 0 & \cdots & 1/N\omega_0 & 0 \\ 0 & 0 & \cdots & 0 & 1/N\omega_0 \end{bmatrix}. \tag{39}$$

Using Equations 23–25, the 2-norm of the amplitude constraint in Equation 38 becomes a function of the vector $P$:

$$\begin{aligned}\left\|\Delta\hat{u}\right\|_2^2 = \frac{T}{2}\big(&P^T H^T W^2 H\, P\\ &- 2\,Q^T\, W^2 H\, P + Q^T W^2 Q\big).\end{aligned} \tag{40}$$

Substituting the Equations 37 and 40 into the Inequalities 33 and 34, the sufficient conditions for satisfaction of the constraints are

$$P^T P \leq \frac{1}{N}F_{max}^2, \tag{41}$$

and

$$\begin{aligned}P^T H^T W^2 H\, P - 2\,Q^T\, W^2 H\, P\\ + Q^T W^2 Q \leq \frac{1}{N}\Delta U_{max}^2,\end{aligned} \tag{42}$$

while the sufficient conditions for constraint's violations are

$$P^T P \geq 2F_{max}^2 \tag{43}$$

and

$$\begin{aligned}P^T H^T W^2 H\, P - 2\,Q^T\, W^2 H\, P\\ + Q^T W^2 Q \geq 2\Delta U_{max}^2.\end{aligned} \tag{44}$$

The Inequalities 41–44 describe the constraints as a function of the PTO force only, in terms of the vector $P$, for given excitations $EA$ and $EB$, embedded in the vector $Q$.

### C. Geometrical interpretation of the constraints

Defining the sets

$$S_f(R_f) = \left\{P : P^T P \leq R_f\right\}, \tag{45}$$

$$S_u(R_u) = \left\{P : P^T H^T W^2 H\, P - 2\, Q^T\, W^2 H\, P + Q^T W^2 Q \leq R_u\right\} \tag{46}$$

a sufficient condition for the satisfaction of both the force and the amplitude constraints described by the Inequalities 29 and 30 is

$$S_f\left(\frac{1}{N} F_{max}^2\right) \cap S_u\left(\frac{1}{N}\Delta U_{max}^2\right) \neq \emptyset, \tag{47}$$

while the sufficient condition for the violation of at least one of the Inequalities 29 or 30 is

$$S_f\left(2F_{max}^2\right) \cap S_u\left(2\Delta U_{max}^2\right) = \emptyset. \tag{48}$$

The force constraint defined by the set $S_f(R_f)$ can be interpreted as the region of the $2N$-dimensional space $S^P$ enclosed by the hypersphere centered in the origin and of radius $\sqrt{R_f}$. The amplitude constraint $S_u(R_u)$ is the region of the space enclosed by the hyperellipsoid with axes parallel to the elements of the basis of $S^P$, because the matrix $H^T W^2 H$ is diagonal and with all positive elements. The center $P_c$ of the ellipsoid is

$$P_c = H^{-1} Q = H^{-1}(Q^A E^A - Q^B E^B), \tag{49}$$

while the radii $r_i$ are given by

$$r_i = \sqrt{\frac{R_u}{\lambda_i}}, \tag{50}$$

where $\lambda_i$ are the eigenvalues of $H^T W^2 H$, that is the diagonal elements.

The Equation 47 states that if the intersection between the hypersphere describing the force constraint and the hyperellipsoid describing the amplitude constraint is not the empty set, then, for the given excitation forces, the device is able to satisfy both the amplitude and the force constraints. Conversely, Equation 48 states that if the intersection between the two sets is the empty set, then at least one constraint will be violated.

In the following section, the procedure for a single body WEC is presented as a special case of the self-reacting WEC; Section III-A explains in greater details the practical significance of Equations 47 and 48.

## III. Single-body point absorber

A single body heaving buoy is now considered as a special case of the self-reacting point absorber described in Section II, given by the frequency domain model

$$(i\omega\, m + B + Z(\omega) + S/i\omega)\, V = F_e - F_{pto}. \tag{51}$$

The corresponding time domain model is

$$L(t) = (m + m_\infty)\dot{v}(t) + k(t) * v(t) + B\, v(t) + S\, u(t) - f_e(t) + f_{pto}(t) = 0, \tag{52}$$

and the energy absorbed by the PTO, neglecting losses, is

$$J(T) = \int_0^T f_{pto}(t)\, v(t)\, dt. \tag{53}$$

Following the same steps performed for the self-reacting device, using a truncated Fourier series to approximate the excitation force, the velocity and the PTO force, as in Equations 9, 11 and 12, and solving

$$\langle L(t), \phi_n \rangle = 0 \quad \forall n = 1, \ldots N, \tag{54}$$

the equation of motion results in the linear system

$$G\, X = E - P. \tag{55}$$

The matrix $G$ is block diagonal with 2-by-2 blocks of the form in Equation 20; the elements on the main diagonal are the real parts of the mechanical impedance at the $N$ frequencies $n\omega_0$, as defined in Equations 16–19. If the matrix $G$ is invertible, the converted energy is

$$J(P) = P^T X = -P^T G^{-1} P + P^T G^{-1} E. \tag{56}$$

where the symmetric part of the matrix $G^{-1}$ is positive definite, because the elements on its main diagonal (linear damping plus radiation resistance) are positive. As a consequence, the quadratic function $J(P)$ is concave and the PTO force $\bar{P}$ that maximizes Equation 56 is

$$\bar{P} = (G^{-T} + G^{-1})^{-1} G^{-1} E. \tag{57}$$

The force constraint is defined as

$$\left\|\hat{f}_{pto}\right\|_\infty \leq F_{max}, \tag{58}$$

and the amplitude constraint is defined as

$$\left\|\hat{u}\right\|_\infty \leq U_{max}. \tag{59}$$

The 2-norm of the force constraint is defined as in Equation 37, while the 2-norm of the amplitude constraint is

$$\left\|\hat{u}\right\|_2^2 = \frac{T}{2}\Big(P^T G^{-T} W^2 G^{-1} P - 2\, E^T G^{-T} W^2 G^{-1} P + E^T G^{-T} W^2 G^{-1} E\Big). \tag{60}$$

### A. Geometrical interpretation of the constraints

Defining the set

$$S'_u(R_u) = \left\{P : P^T G^{-T} W^2 G^{-1} P - 2\, E^T G^{-T} W^2 G^{-1} P + E^T G^{-T} W^2 G^{-1} E \leq R_u\right\}, \tag{61}$$

a sufficient condition for the satisfaction of both the force and the amplitude constraints defined by the Inequalities 58 and 59 is

$$S_f\left(\frac{1}{N} F_{max}^2\right) \cap S'_u\left(\frac{1}{N} U_{max}^2\right) \neq \emptyset \tag{62}$$

and a sufficient condition for the violation of at least one constraint is

$$S_f\left(2F_{max}^2\right) \cap S'_u\left(2U_{max}^2\right) = \emptyset. \tag{63}$$

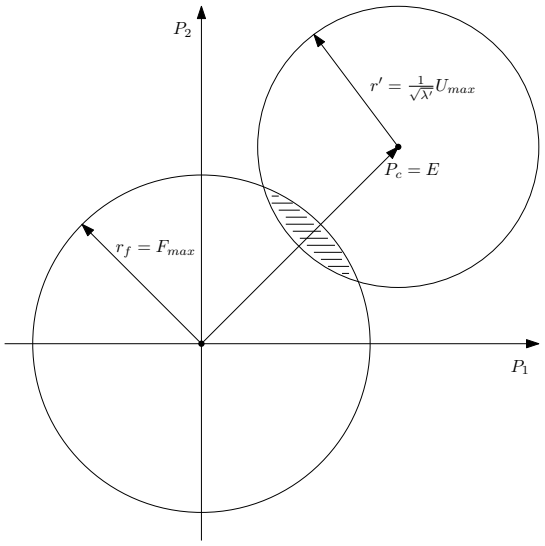


Fig. 2. Example for one-body device, with $N$=1. The intersection is not empty (shaded region), thus the sufficient condition in Equation 62 is satisfied. The axes $P_1$ and $P_2$ are the components of the vector $P$ describing the PTO force, that is $P = [P_1\ P_2]^T$.

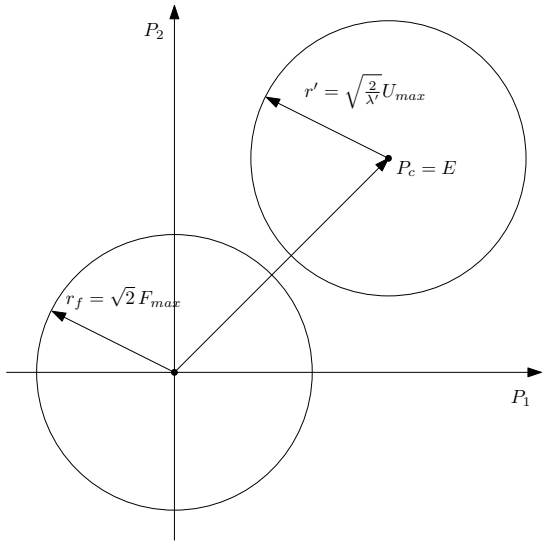


Fig. 3. Example for one-body device, with $N$=1. The intersection is empty, thus at least one constraint will be violated. The axes $P_1$ and $P_2$ are the components of the vector $P$ describing the PTO force, that is $P = [P_1\ P_2]^T$.

The set $S'_u(R_u)$ describes the region of the space $S^P$ enclosed by an hyperellipsoid centered at $P_c$=$E$; the principal axes are parallel to the elements of the basis because the matrix $G^{-T}W^2G^{-1}$ is diagonal and the radii are

$$r'_i = \sqrt{\frac{R_u}{\lambda'_i}}, \tag{64}$$

where $\lambda'_i$ are the eigenvalues of $G^{-T}W^2G^{-1}$.

An example for $N$=1 (i.e. 2-dimensions, $P_1$ and $P_2$) is shown in Fig. 2; the matrix $G^{-1}$ is of the form in Equation 20, thus $G^{-T}W^2G^{-1}$ is diagonal with two coincident eigenvalues $\lambda'$, and the set $S'_u(U^2_{max})$ is a disc centered at $P_c$=$E$ with radius $r'$=$U_{max}/\sqrt{\lambda'}$ . Considering that the intersection between two disks is non empty if the sum of the radii is larger that the distance between the centers, it follows that the sufficient condition in Equation 62 can be simplified as:

$$F_{max} + \frac{U_{max}}{\sqrt{\lambda\prime}} \geq \left\|E\right\|_2. \tag{65}$$

A further example, also for $N$=1, is depicted in Fig. 3; a situation is shown in which the intersection between the regions describing the sufficient conditions for the violation of at least one constraint, expressed by Equation 63, is empty; in this case, for the given excitation $E$, at least one constraint will be violated. Equation 63, for $N$=1, can be simplified to:

$$\sqrt{2}\left(F_{max} + \frac{U_{max}}{\sqrt{\lambda\prime}}\right) \leq \left\|E\right\|_2. \tag{66}$$

## IV. Illustrative example and discussion on the method's application

The introduction of the 2-norm for the description of the force and amplitude constraints allows the study of their properties analytically. The analysis is not exact, in the sense that the sufficient conditions described by Equations 47 and 62 are conservative, and the device might satisfy both constraints (Inequalities 29–30 and 58–59) even if Equations 47 and 62 are not true. In practice, during the design of the WEC, the Equations 47 and 62 provide an estimate of the requirements for the mechanical components of the device. In particular, the necessary conditions in Equations 48 and 63 describe the minimum requirements that a WEC has to meet for a particular sea spectrum described by the excitation $E$. In other words, if Equations 48 and 63 are not satisfied, then the WECs will definitely not be able to satisfy both constraints at the same time for the given excitation $E$. When considering one frequency at the time ($N$=1), the formulation of the constraints presented in Sections II and III can be visualized in a 2-D plot, as in Fig. 2 and Fig. 3. For a higher dimension ($N$>2), the Equations 47, 48, 62, and 63 require the analysis of the intersection of a hypersphere with a hyperellipsoid, which can be studied using numerical methods only, although it is not a difficult problem because both the hypersphere and the hyperellipsoid are convex surfaces. Some analysis of the constraint's requirements can still be carried out by considering the largest hyperspheres contained in each of the ellipsoids and the smallest hyperspheres that contain each of the ellipsoids. In this case, an estimate of the approximation is provided by the ratio $r_{max}/r_{min}$, where $r_{max}$ and $r_{min}$ are the largest and the smallest radii of the hyperellipsoid, as defined in Equations 50 and 64.

The first step for the practical implementation of the method is to build the matrix $G$ which is used to calculate the radii $r_i$ and $r'_i$ and the center $P_c$ of the hyperellipsoid describing the amplitude constraint. In the case of a self-reacting WEC, $G$ is composed of four blocks $G^{ij}$ (Equation 14), each of which is block diagonal (Equation 15) and their elements are calculated

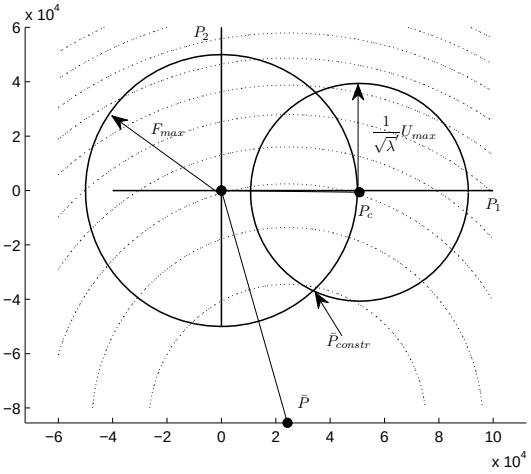


Fig. 4. Example for one-body device with $N$=1, $F_{max}$=50kN, $U_{max}$=3m, $T$=9s.

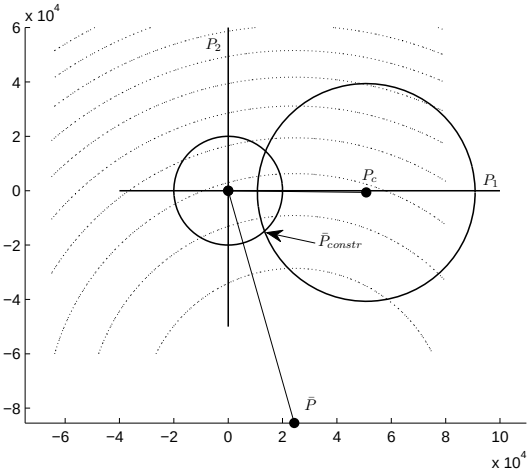


Fig. 5. Example for one-body device with $N$=1, $F_{max}$=20kN, $U_{max}$=3m, $T$=9s.

directly from the frequency domain hydrodynamic coefficients of the bodies composing the device, by using Equations 16–19. If only one frequency component $\omega_0$ is considered (i.e. $N$=1), then the matrix $G$ is 4-by-4 and its structure is given explicitly by Equation 21, with $n$=1. Once $G$ has been built, the radii $r_i$ can be calculated directly (Equation 50) from the elements $\lambda_i$ of the diagonal matrix $H^T W^2 H$ , where $W$ is defined in Equation 39 and $H$ is obtained by combining the blocks $G^{ij}$, as described by Equation 23. The center of the hyperellipsoid $P_c$ (Equation 49) depends on the matrices $Q^A$ and $Q^B$, that are by calculated from the block $G^{ij}$ (Equations 26 and 27 ), and on the vectors of the Fourier coefficients of the excitation forces $E^A$ and $E^B$, defined in Equations 12 and 13. If only one frequency at the time is considered ($N$=1), then the hyperellipsoid is a circle, the matrix $H^T W^2 H$ is 2-by-2 and the diagonal elements are equal, that is $\lambda_1$=$\lambda_2$=$\lambda$.

In the case of a single body WEC, the procedure is simpler in that the matrix $G$ corresponds exactly to the one described

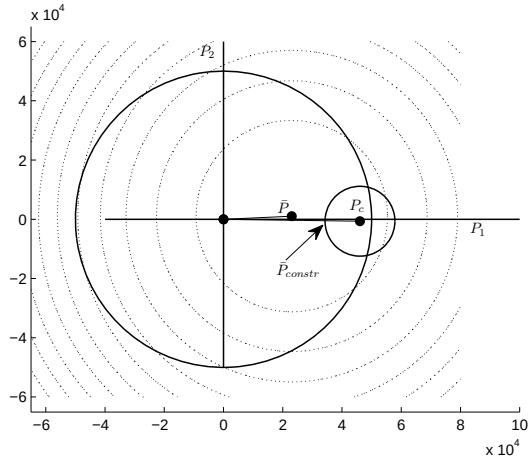


Fig. 6. Example for one-body device with $N$=1, $F_{max}$=50kN, $U_{max}$=3m, at resonance: the optimum PTO force is in phase with the excitation force.

in Equation 15 setting $i$=$j$, that is $G$=$G^{ii}$. Only Equations 16 and 17 are needed to calculate the elements of $G$ since the cross-coupling terms ($i \neq j$) are not present. The radii of the hyperellipsoid $r_i'$ are calculated directly from the diagonal elements of the matrix $G^{-T} W^2 G^{-1}$ by using Equation 64, while the position of the center $P_c$ is equal to $E$, that is the vector of the Fourier coefficients of the excitation force. When only one frequency component at the time is considered ($N$=1), the matrix $G$ is 2-by-2 and the amplitude constraint is described by a circle centered in $E$; for the case of the sufficient condition for constraints satisfaction (Fig. 2), its radius is $r'$=$U_{max}/\sqrt{\lambda'}$, that is obtained setting $R_u$=$U_{max}^2$ in Equation 64, while the radius of the circle describing the force constraint is $r_f$=$F_{max}$ (Equation 62). When considering the sufficient condition for the violation of at least on constraint (Fig. 3), the radius of the circle relative to the amplitude constraint is $r'$=$\sqrt{2/\lambda'}U_{max}$, that is obtained setting $R_u$=$2U_{max}^2$ in Equation 64, while the radius of the circle describing the force constraint is $r_f$=$\sqrt{2}F_{max}$ (Equation 63).

Besides the analysis of the violation of the constraints, it is also possible to study the effect of constraints on the energy absorbed by the PTO. Figures 4 and 5 shows the sufficient conditions for constraint satisfaction relative to the same device, a vertical cylinder with radius 5m and draft 25m, subject to the same monochromatic wave profiles, but with different force constraints. The vector $\bar{P}$ corresponds to the optimal PTO force provided by Equation 57, while $P_c$ is the center of the disc describing the amplitude constraint, as depicted in Fig 2. The circular dotted lines centered in $\bar{P}$ are the contour lines corresponding to constant absorbed energy. The maximum energy absorbed, while satisfying the constraints, is achieved for $P$=$\bar{P}_{constr}$; for the situation depicted in Fig. 4, where $F_{max}$=50kN, increasing $F_{max}$ will provide a small increase on the absorbed energy, because $\bar{P}_{constr}$ will move along the circle described by the amplitude constraint, and the tangent to that circle at that point is almost parallel with the contour lines. Increasing $U_{max}$ by the same amount, in percentage terms,

will provide a larger increase, because $\bar{P}_{constr}$ will move along the circle described by the force constraint, which is almost orthogonal to the contour lines. The situation is completely the opposite in Fig 5, where $F_{max}$= 20kN; in this case, the larger increase in the absorbed energy is provided by the increasing $F_{max}$.

The situation in Fig. 6 corresponds to the resonance frequency of the vertical cylinder, which can be seen by the fact that the optimal PTO force is in phase with $P_c$ which is, for the single body case, equal to the excitation $E$. In this case, a variation in $F_{max}$ has no effect on the amount of absorbed energy, because the only active constraint in $P_{constr}$ is the one due to the amplitude.

The radius of the circle relative to the amplitude constraints at resonance is smaller than the same radius at $T$=9s (Fig. 4); this is due to the fact that $r' = 1/\sqrt{\lambda'}U_{max}$, and $\lambda'$ takes its largest value at resonance. In fact, it can be verified by using Equations 16–19 that $\lambda'$ is inversely proportional to the magnitude of the mechanical impedance of the device.

The procedure described in sections II and III provides results on the conditions for satisfaction of the constraints that can be obtained directly using the theory currently available in text books, such as [1]. However, the discretization allows the study of the constrains in a finite dimensional vector space, giving the possibility to interpret their meaning from an intuitive point of view, (i.e. geometrical objects), and allowing the use of the wide range of tools available for this mathematical structure. Furthermore, the discretization of the equations of motion by means of the Fourier series is just a special case. Different basis functions can be used in Equations 5 and 6, providing different conditions for the satisfaction and violation of the constraints, which can still be interpreted as geometrical objects. The cost function describing the energy absorbed by the PTO in Equation 22 will still be quadratic with respect to the vector $P$.

## V. Conclusion

This paper presents a procedure for the analysis of the force and amplitude constraints on a self-reacting point absorber; the special case of a single body in also considered. Sufficient conditions for the satisfaction of both constraints and/or the violation of at least one constraint have been identified. The viability of a PTO system or a device geometry is quickly verified, for specific sea states, by means of a few linear algebra operations, avoiding the time consuming task of numerically integrate the equations of motion.

If reliable estimates for the economic cost of the PTO capacity, namely $F_{max}$ and $U_{max}$, are available, the sensitivity of the absorbed energy with respect to the maximum PTO force and to the maximum oscillation amplitude, described in section IV, could also be useful in the techno-economical optimization of the device.

For these reasons, we envisage this method being a useful tool in the design stage, in particular prototyping and optimization, of wave energy converters.

## Appendix

The 2-norm $\|f\|_2$ of the function $f(t)$ is defined as

$$\left\|f\right\|_2 = \left(\int_0^T |f(t)|^2 dt\right)^{1/2}, \tag{67}$$

while the infinity-norm $\|f\|_\infty$ is defined as

$$\left\|f\right\|_\infty = \sup_{t\in[0,T]} |f(t)|. \tag{68}$$

A general property relating the 2-norm and the infinity-norm of a function $f$, for which the norm defined by Equation 68 exists, is [6]

$$\left\|f\right\|_2 \leq \sqrt{T}\left\|f\right\|_\infty. \tag{69}$$

For a zero mean Fourier series with $N$ frequency components the inequality [7]

$$\left\|f_N\right\|_\infty \leq \sqrt{\frac{2N}{T}}\left\|f_N\right\|_2 \tag{70}$$

provides an upper bound for the infinity-norm as a function of the 2-norm.

## Acknowledgment

The authors gratefully acknowledge the financial support of Enterprise Ireland under contract EI/CTFD/2006/IT/325.

## References

[1] J. Falnes, *Ocean waves and oscillating systems: linear interactions including wave-energy extraction*. Cambridge University Press, 2002.

[2] G. Bacelli, J. V. Ringwood, and J.-C. Gilloteaux, "A control system for a self-reacting point absorber wave energy converter subject to constraints," in *IFAC World Congress*, 2011.

[3] J. Falnes, "Wave-energy conversion through relative motion between two single-mode oscillating bodies," *Journal of Offshore Mechanics and Arctic Engineering*, vol. 121, no. 1, pp. 32–38, 1999. [Online]. Available: http://link.aip.org/link/?JOM/121/32/1

[4] T. Ogilvie, "Recent progress toward the understanding and prediction of ship motions," in *Proc. Fifth Symposium on Naval Hydrodynamics, Bergen, Norway*, 1964.

[5] J. P. Boyd, *Chebyshev and Fourier Spectral Methods*. Dover, 2001.

[6] K. Atkinson and W. Han, *Theoretical Numerical Analysis: A Functional Analysis Framework*. Springer, 2005.

[7] A. F. Timan, *Theory Of Approximation Of Functions Of A Real Variable*. Courier Dover Publications, 1994.